

# Noncovalent Stable Functionalization Makes Carbon Nanotubes Hydrophilic and Biocompatible

Friederike Ernst,<sup>\*,†</sup> Zhenghong Gao,<sup>‡,§</sup> Raúl Arenal,<sup>||,⊥</sup> Timm Heek,<sup>#</sup> Antonio Setaro,<sup>†</sup> Rodrigo Fernandez-Pacheco,<sup>||</sup> Rainer Haag,<sup>#</sup> Laurent Cognet,<sup>‡,§</sup> and Stephanie Reich<sup>†</sup>

<sup>†</sup>Institut für Experimentalphysik, Freie Universität Berlin, Arnimallee 14, 14195 Berlin, Germany

<sup>‡</sup>LP2N, University of Bordeaux, UMR 5298, 351 cours de la libération, F-33405 Talence, France

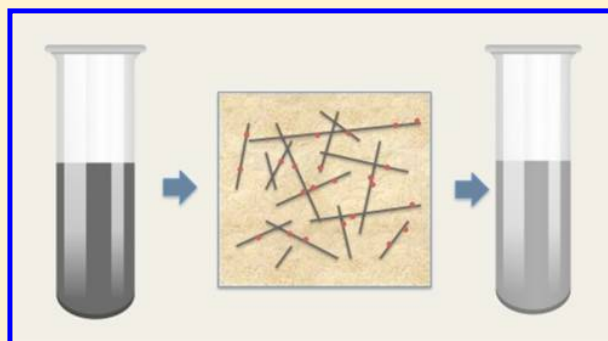
<sup>§</sup>Institut d'Optique & CNRS, UMR 5298, F-33405 Talence, France

<sup>||</sup>Laboratorio Microscopias Avanzadas (LMA), Inst. Nanociencia Aragon (INA), University of Zaragoza, Zaragoza 50018, Spain

<sup>⊥</sup>Fundacion ARAID, Zaragoza 50018, Spain

<sup>#</sup>Institut für Chemie und Biochemie, Freie Universität Berlin, Takustraße 3, 14195 Berlin, Germany

**ABSTRACT:** Semiconducting single-wall carbon nanotubes possess an intrinsic photoluminescence in the near-infrared region beyond 900 nm, the NIR-II window of biological imaging. Here, we introduce a modular molecule for noncovalent nanotube functionalization which renders carbon nanotubes hydrophilic and fully biocompatible through a one-step process. We demonstrate through electron energy-loss spectroscopy (EELS) spectroscopy that the noncovalent functionalization mechanism relies on tight and extremely robust  $\pi$ - $\pi$  stacking, which survives an exchange of the solvent as well as drying. Furthermore, the modularity of the molecule design allows for the introduction of functional units into the molecule itself to modify the optical properties of the carbon nanotube, for instance to augment its excitation window through an excitation energy transfer, facilitating the excitation of most carbon nanotube chiralities at one single wavelength.



## INTRODUCTION

Single-wall carbon nanotubes are becoming popular for biomedical applications for several reasons: They are small, chemically stable, hollow, and fillable, have a large absorption cross section, and lend themselves to chemical functionalization.<sup>1,2</sup> Consequently, they can be used as cargo vessels to release drugs in a precise location in a cell or in the body<sup>3,4</sup> and to locally convert electromagnetic radiation into heat in photothermal therapy<sup>5,6</sup> and can be functionalized with antibodies and a plethora of other attachments to be used as sensors.<sup>7,8</sup> Carbon nanotubes also possess optoelectronic properties that make them a highly desirable candidate for biological imaging.<sup>9,10</sup> The intrinsic luminescence emission of single-wall carbon nanotubes lies in the near-infrared region from 900 to 1400 nm, the second optical window of tissue. Biological tissues are relatively transparent between 650 and 1350 nm. However, in practice, the first optical window between 650 and 950 nm for which there are well-established biocompatible fluorophores is obscured by tissue autofluorescence.<sup>11</sup> The second optical window between 1000 and 1350 nm has been demonstrated to exhibit 100-fold improved signal-to-noise ratios when imaging whole animals as compared to the first window, making carbon nanotube based systems with an

intrinsic luminescence in the NIR highly desirable for biomedical imaging.<sup>12–14</sup>

Carbon nanotubes are intrinsically hydrophobic and have a propensity for bundling. For applications in biomedical imaging nanotubes require solubilization through noncovalent functionalization with amphiphilic surfactants. Using small molecules in carbon nanotube solubilization has the distinct advantage that the molecule's design is flexible and can easily be modified to incorporate additional functionalities. The biocompatibility of small surfactant–nanotube hybrids faces three challenges.

- (i) The surfactant has to suspend nanotubes in a wide range of pHs, reflecting the variable environments encountered in biological tissues.
- (ii) The surfactant ought not interact with the surrounding cellular environment itself and preclude interaction between nanotube and environment as well.
- (iii) The dynamic equilibrium between adsorbed and free surfactant must be strongly in favor of the adsorbed state. This stability is important not only for the sake of

**Received:** March 31, 2017

**Revised:** June 10, 2017

**Published:** August 3, 2017



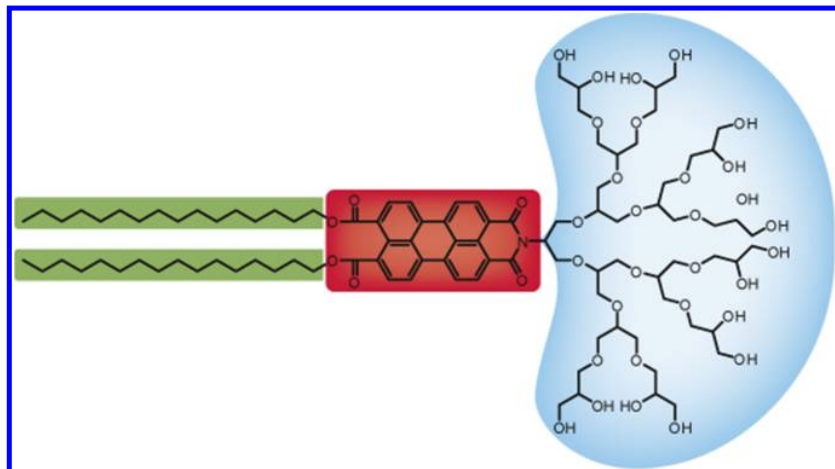


**Figure 1.** PerPG is a small amphiphilic molecule which serves as a biocompatible surfactant for carbon nanotubes. PerPG comprising three functional parts: hydrophilic polyglycerol (PG) dendron for water solubility (blue), perylene-derived dye core for attachment to the nanotube (red), and alkyl chains for nanotube individualization (green).

continued suspension but also because the surfactant shields the environment against the nanotube.

We recently introduced an amphiphilic molecule for functionalizing carbon nanotubes, PerPG. PerPG forms tightly bound complexes with carbon nanotubes, in effect serving as a surfactant in solution. Instead of a charged headgroup, PerPG possesses a hydrophilic polyglycerol (PG) dendron.<sup>15</sup> PG dendrons are known to interact with proteins very weakly and are consequently popular as a protein-repellent coating, for instance in antifouling surfaces.<sup>16–19</sup> We combine the PG dendron with two parallel alkyl chains for nanotube individualization and a perylene diimide dye. The perylene-derived dye forms ultraefficient energy transfer complexes with the nanotube.<sup>15,20</sup> This energy transfer functionality enables the excitation of all nanotube chiralities at one single wavelength, possibly potentiating their use in biomedical sensing, imaging, and photothermal therapy applications.

Here, we present high-resolution transmission electron microscopy (HRTEM) and electron energy-loss spectroscopy (EELS) data confirming that. The nanotube–PerPG complexes are highly stable and robust against change of medium and drying. We assess PerPG’s biocompatibility by performing a cell viability study and find that at relevant concentrations the small designer molecules are as biocompatible as conventionally used biocompatible poloxamers such as pluronic.<sup>21</sup>

## RESULTS AND DISCUSSION

**Imaging of Nanotube–PerPG Hybrids.** PerPG, shown in Figure 1, solubilizes nanotubes efficiently in aqueous solution and forms energy transfer complexes with the carbon nanotubes.<sup>15</sup> Its design is modular in nature, comprising alkyl chains for nanotube individualization (green), a pH-independent PG dendron for water solubility (blue), and a functional perylene unit (red), which is the donor unit in the energy transfer complexes formed with the nanotubes. The combination of these three building blocks was previously systematically varied and optimized for both energy transfer and nanotube suspension capabilities.<sup>22</sup> The suspension was further optimized for negligible free surfactant and stability through absorption and photoluminescence measurements.<sup>15</sup> The energy transfer is FRET-like with an efficiency on the order of 99.99%. In

conjunction with the spectral overlap between donor emission and acceptor absorption we calculate the distance between nanotube and dye in a point-dipole approximation to be 0.7 nm.<sup>20</sup> However, the point-dipole approximation overestimates the distance between donor and acceptor in this case, as an exciton in the nanotube is not well described as a point-dipole. Instead, the dipole is oblong, decreasing the interaction with the point-dipole of the dye. Consequently, for a given interaction strength, the point-dipole approximation overestimates the distance between dye and nanotube.<sup>23</sup> Based on this, the upper limit for the distance between the nanotube and dye unit is 0.7 nm, only slightly more than for van der Waals bound systems. Hence we assumed that the extended  $\pi$ -orbitals of the carbon nanotube interact with the extended  $\pi$ -orbitals of the perylene derivative dye, resulting in an adsorption of the dye on the tube wall through a  $\pi$ – $\pi$  stacking mechanism.<sup>20,23,24</sup> The coverage rate depends slightly on the nanotube chirality and was previously estimated to be on the order of 0.1 through a detailed analysis of absorption, photoluminescence, and photoluminescence excitation measurements of the carbon nanotube–PerPG complexes.<sup>20</sup>

To confirm the adsorption of PerPG on the nanotube surface, we perform a high-resolution TEM study. HRTEM micrographs show microcrystalline regions on top of the nanotubes (Figure 2). These microcrystalline structures are shown to be PerPG in subsequent EELS measurements (Figure 3). Spatially resolved EEL spectroscopy is an ideal technique to gain insight into the morphology of the nanotube–PerPG complexes, letting us directly visualize the organic biomolecules on top of the nanotube through the evaluation of the local chemical composition.<sup>25,26</sup> Particular attention was paid to reducing the beam dose used to optimize the acquisition conditions (see Experimental Section). Figure 3B shows EEL spectrum lines recorded on a bundle of functionalized carbon nanotubes. The locations of the spectral acquisitions are given in Figure 3A, the corresponding high-angular annular dark field (HAADF) scanning transmission electron microscopy (STEM) image. In the HAADF image we see a bright area of  $\sim 5 \times 1.5$  nm<sup>2</sup> in the middle of the nanotube bundle. Other regions like the one indicated are also visible. These brighter appearing moieties are localized at the surface of the nanotubes as we have observed in the HRTEM micrographs (Figure 2). The EEL

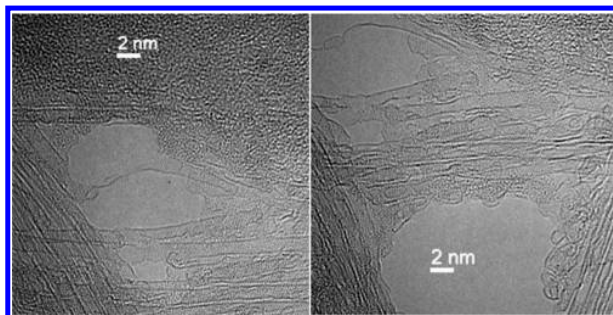


**Figure 2.** High-resolution transmission electron micrographs of nanotube–PerPG hybrids. The PerPG molecules can be seen as faint microcrystalline regions superimposed on the nanotubes as confirmed by EELS measurements (see Figure 3).

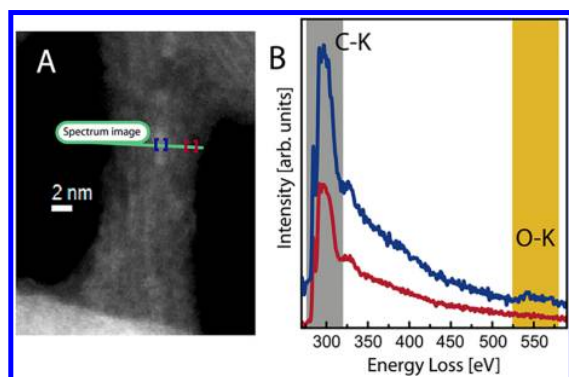


**Figure 3.** (A) HAADF image of a bundle of functionalized carbon nanotubes. EELS data were acquired along the green line. (B) Sums of 5 EEL spectra collected from two different areas, marked in blue and red. While the C–K edge is visible in both spectra, the O–K edge is only visible in the blue (top) EEL spectrum acquired in the bright area of the HAADF image.

spectrum line was acquired following the green line marked in Figure 3A, which crosses this bright region. The sum of 5 EEL spectra was extracted from the two areas marked in the HAADF image (Figure 3B). Both EEL spectra display the C–K edge with the characteristic peaks of  $sp^2$  materials at 285 and 292 eV corresponding to the  $\pi^*$  and  $\sigma^*$  contributions, respectively.<sup>25–30</sup> In the spectrum acquired over the bright region in the HAADF micrograph we additionally detect oxygen (see Figure 3B): The O–K edge is clearly visible, as designated on the graph. The amount of oxygen in this region, obtained from the analysis of this EEL spectrum, is  $\sim 14\%$ . The combination of the HRTEM images and local analytical findings confirms that the perylene unit of PerPG  $\pi$ – $\pi$  stacks on the nanotube wall, resulting in extremely tight binding between nanotube and the small amphiphilic molecule.

We would like to draw special attention to the fact that the nanotube–PerPG complexes were created in aqueous solution, resulting in well-individualized nanotubes as attested to by strong PL emission.<sup>15</sup> The aqueous sample was subsequently dried and then redispersed in ethanol for these measurements (Figure 4). This means the complexes are bound tightly enough to remain bundled throughout the drying process. Furthermore, they are stable in air and highly robust with respect to change of the environment, indicating that this PerPG–nanotube complex may be bound tightly enough to satisfy

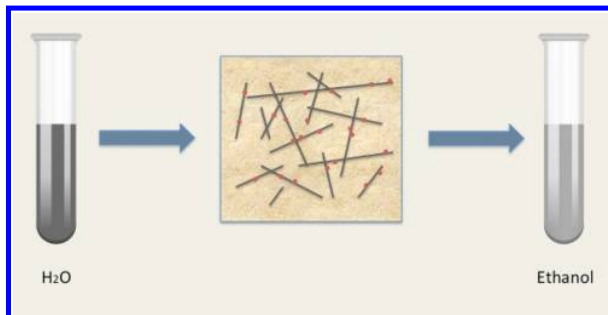


**Figure 4.** Carbon nanotube–PerPG complexes created in aqueous solution remain stable through the process of drying and redispersion in ethanol.

challenges (i) and (iii) of achieving biocompatibility for small surfactant–nanotube hybrids.

**Suitability for Biomedical Applications.** We designed PerPG such that it is tailored for use in biomedical applications. Regarding the three challenges (i)–(iii) of biocompatibility discussed in the Introduction, challenge (i) pH independence and (ii) weak interaction with surrounding tissue are met by the polyglycerol dendron as a hydrophilic unit. The PG dendron’s hydrophilicity is a result of its multiple oxygen bonds, not of the presence of a charged salt. All bonds are fully saturated and much less susceptible to deprotonation upon pH variation. PG dendrons have been previously reported to not interact with proteins as necessary to meet challenge (ii).<sup>16–19</sup> Challenge (iii), a strong preference toward the adsorbed over the free state, is tackled by the adsorption mechanism of PerPG as we verify from the absence of perylene luminescence. The emission of the perylene dye in the PerPG is quenched when it is in close contact with a nanotube. Residual dye emission is an excellent measure of free PerPG. The residual emission is quenched by a factor of  $10^4$ , corresponding to a ratio of adsorbed to free molecules of 10 000:1 or higher.<sup>15</sup> This remarkably high ratio of adsorbed to free PerPG is attributed to the strong  $\pi$ – $\pi$  stacking exhibited between the  $sp^2$ -bonded carbon network of the nanotube and the organic perylene moiety. This agrees with the HRTEM and EELS studies that highlighted the stability of the complexes with respect to drying and redispersal in another medium.

We assess the biocompatibility of PerPG suspended nanotubes by a cell viability study. To access cell viability we conduct an MTT assay after exposure to the nanotube–PerPG hybrids.<sup>31</sup> It measures the activity of cellular enzymes in metabolically active cells. The enzymes reduce yellow tetrazolium dyes into its insoluble, purple formazan that can be solubilized and quantified by spectrophotometric means. The MTT assay is widely accepted as a sensitive and reliable tool in assessing cytotoxicity.<sup>31</sup>

Carbon nanotubes suspended in PerPG are added to COS-7 cell cultures with a final nanotube concentration of 0.1  $\mu\text{g}/\text{mL}$ , 0.1  $\mu\text{g}/\text{mL}$  being the highest concentration that may be used for applications in single nanotube imaging and tracking. PerPG is benchmarked against Pluronic as a standard surfactant to make nanotubes biocompatible.<sup>21</sup> The relative cell viability (Figure 5A) demonstrated that PerPG is equally biocompatible as Pluronic. Figure 5B reports the cell viability of PerPG-suspended nanotubes for different nanotube concentrations ranging from  $1 \times 10^{-3}$   $\mu\text{g}/\text{mL}$  to 1  $\mu\text{g}/\text{mL}$ . The biocompatibility of the suspended nanotubes increases

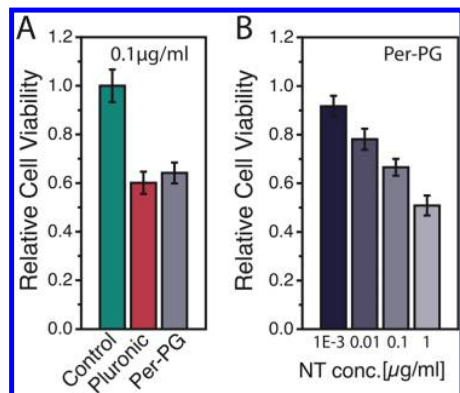


**Figure 5.** Relative cell viability as measured in an MTT assay for different surfactants and NT concentrations. (A) Relative cell viability after exposure to nanotubes suspended with Pluronic and PerPG at a nanotube concentration of 0.1  $\mu\text{g}/\text{mL}$ . The control group was subjected to the same treatments without addition of nanotubes. (B) Relative cell viability for different concentrations of PerPG-suspended nanotubes.

drastically with lowered concentration reaching 90% viability at  $10^{-3}$   $\mu\text{g}/\text{mL}$ . PerPG thus reached the same performance as the polymeric biocompatible surfactant Pluronic, demonstrating that it is well suited as a biocompatible surfactant for nanotubes.

## EXPERIMENTAL SECTION

**Sample Preparation.** An amount of 0.11g/L of HiPco SWNTs (Unidym, batch SP029S) was dispersed with  $6 \times 10^{-5}$  M of PerPG or Pluronic through tip sonication with a Bandelin SonoPlus HD 2070 with 30% of the maximum power of 70 W and a 3 mm microtip. The sample was subsequently centrifuged at 30 000g and 23° for 90 min. Only the supernatant was used in the experiments. The synthesis of PerPG is published.<sup>15</sup>

**HRTEM and EELS.** The transmission electron microscopy (TEM) samples were prepared by redispersing the dried nanotube–PerPG complexes in ethanol. The dispersions were ultrasonicated and subsequently deposited on holey carbon 3 mm copper grids. High-resolution TEM was performed employing an imaging-side aberration-corrected FEI Titan-Cube microscope working at 80 keV, equipped with a Cs corrector (CETCOR from CEOS GmbH).

Spatially resolved electron energy loss spectroscopy (EELS) measurements were performed on probe-corrected scanning TEM (STEM) FEI Titan Low-Base 60–300 operating at 80 keV (fitted with a X-FEG gun and Cs-probe corrector (CESCOR from CEOS GmbH)). EEL spectra were recorded using the spectrum-imaging (SPIM in 2D or spectrum-line (SPLI) in 1D) mode<sup>32,33</sup> in a Gatan GIF Tridiem ESR 865 spectrometer. The convergent semiangle was 25 mrad, and the collection semiangle 80 mrad had an energy resolution  $\sim 1.2$  eV.

**Cell Viability Study.** COS-7 cells are seeded in a 96-well plate with 100  $\mu\text{L}$  of COS-7 solution ( $2.5 \times 10^4$  cells/mL) in each well and cultured at 37 °C and 5%  $\text{CO}_2$  for 24 h. An amount of 11  $\mu\text{L}$  of SWNT suspension (1  $\mu\text{g}/\text{mL}$ ) is added to each well, resulting in a final concentration of 0.1  $\mu\text{g}/\text{mL}$ . Cultures are kept at 37 °C and 5%  $\text{CO}_2$  for a further 24 h. Subsequently, a 10  $\mu\text{L}$  MTT kit is added to each well, followed by 3.5 h incubation at 37 °C in the dark for reaction. All medium is carefully removed, and 150  $\mu\text{L}$  of MTT solvent is

added into each well; the plate is then wrapped with aluminum paper to isolate from light and put on a laboratory shaker (60 rpm) for thoroughly dissolving MTT reduction. Absorptions were measured with a plate reader (PLUOstar Omega) at 570 nm, the fingerprint region for viable cells, and background is subtracted. The control culture was treated the same without adding SWNT suspension. All data were normalized by the control average.

## CONCLUSIONS

In this paper, we show that a small functional molecule with a modular design, PerPG, is capable of suspending carbon nanotubes in biological surroundings. HRTEM imaging and EEL spectroscopy demonstrate that PerPG adsorbs to the nanotube with its perylene unit, confirming deductions made from earlier photoluminescence measurements. The HRTEM data also confirm the physical robustness of the nanotube–PerPG complexes to drying and solvent exchange and prove the complexes are stable in air, a result of the exceptionally strong binding interaction between nanotube and PerPG’s perylene moiety. A polyglycerol dendron known for low levels of interaction with proteins was chosen for the hydrophilic part of PerPG to achieve biocompatibility of the nanotube complexes. Cell viability is demonstrated by an MTT assay. At concentrations relevant for biotechnological applications the nanotube–PerPG complexes are equally biocompatible as nanotubes suspended in the biocompatible standard surfactant, pluronic F108. Until now, research into nanotube surfactants with a low cytotoxicity has concentrated on polymers. The modularity of the design of the small-molecule surfactant is inherently flexible and could accommodate many other functionalities besides the energy transfer exhibited by PerPG in this manuscript. Tailored small functional molecules that efficiently act as surfactants have the potential to play a significant role in the solubilization of carbon nanotubes for biomedical applications.

## AUTHOR INFORMATION

### Corresponding Author

\*E-mail: [f.ernst@fu-berlin.de](mailto:f.ernst@fu-berlin.de).

### ORCID

Friederike Ernst: 0000-0002-4150-1288

Raúl Arenal: 0000-0002-2071-9093

Rainer Haag: 0000-0003-3840-162X

### Author Contributions

The manuscript was written through contributions of all authors. All authors have given approval to the final version of the manuscript.

### Notes

The authors declare no competing financial interest.

## ACKNOWLEDGMENTS

We gratefully acknowledge the financial support of the European Research Council (grant number 210642) and the German Research Foundation (DFG via SFB 658, subprojects A6 and B7). ZG and LC thank J. Varuela and L. Groc for the use of the absorption reader for MTT assay and acknowledge financial support from CNRS, Agence Nationale de la Recherche (ANR-14-OHRI-0001-01), IdEx Bordeaux (ANR-10-IDEX-03-02), and the France-BioImaging national infrastructure (ANR-10-INBS-04-01). The microscopy works were conducted in the Laboratorio de Microscopias Avanzadas at the

Instituto de Nanociencia de Aragon - Universidad de Zaragoza (Spain). R.A. gratefully acknowledges the support from the Spanish Ministry of Economy and Competitiveness (MINECO) through project grant FIS2013-46159-C3-3-P and MAT2016-79776-P (AEI/FEDER, UE). The Government of Aragon and the European Social Fund are gratefully acknowledged. R.A. gratefully acknowledges the project "Construyendo Europa desde Aragon" 2014-2020 (grant number E/26).

## REFERENCES

- (1) Liu, Z.; Tabakman, S.; Welsher, K.; Dai, H. Carbon Nanotubes in Biology and Medicine: In Vitro and in Vivo Detection, Imaging and Drug Delivery. *Nano Res.* **2009**, *2*, 85–120.
- (2) Kruss, S.; Hilmer, A. J.; Zhang, J.; Reuel, N. F.; Mu, B.; Strano, M. S. Carbon Nanotubes as Optical Biomedical Sensors. *Adv. Drug Delivery Rev.* **2013**, *65*, 1933–1950.
- (3) Bartholomeusz, G.; Cherukuri, P.; Kingston, J.; Cognet, L.; Lemos, R.; Leeuw, T. K.; Gumbiner-Russo, L.; Weisman, R. B.; Powis, G. In Vivo Therapeutic Silencing of Hypoxia-Inducible Factor 1 Alpha (HIF-1 $\alpha$ ) Using Single-Walled Carbon Nanotubes Noncovalently Coated with siRNA. *Nano Res.* **2009**, *2*, 279–291.
- (4) Bianco, A.; Kostarelos, K.; Prato, M. Applications of Carbon Nanotubes in Drug Delivery. *Curr. Opin. Chem. Biol.* **2005**, *9*, 674–9.
- (5) Chakravarty, P.; Marches, R.; Zimmerman, N. S.; Swafford, A. D. E.; Bajaj, P.; Musselman, I. H.; Pantano, P.; Draper, R. K.; Vitett, E. S. Thermal Ablation of Tumor Cells with Antibody-Functionalized Single-Walled Carbon Nanotubes. *Proc. Natl. Acad. Sci. U. S. A.* **2008**, *105*, 8697–8702.
- (6) Kam, N. W. S.; O'Connell, M.; Wisdom, J. A.; Dai, H. Carbon Nanotubes as Multifunctional Biological Transporters and Near-Infrared Agents for Selective Cancer Cell Destruction. *Proc. Natl. Acad. Sci. U. S. A.* **2005**, *102*, 11600–11605.
- (7) Barone, P. W.; Baik, S.; Heller, D. A.; Strano, M. S. Near-Infrared Optical Sensors Based on Single-Walled Carbon Nanotubes. *Nat. Mater.* **2005**, *4*, 86–92.
- (8) Chen, Z.; Tabakman, S. M.; Goodwin, A. P.; Kattah, M. G.; Daranciang, D.; Wang, X.; Zhang, G.; Li, X.; Liu, Z.; Utz, P. J.; et al. Protein Microarrays with Carbon Nanotubes as Multicolor Raman Labels. *Nat. Biotechnol.* **2008**, *26*, 1285–92.
- (9) Welsher, K.; Liu, Z.; Daranciang, D.; Dai, H. Selective Probing and Imaging of Cells with Single Walled Carbon Nanotubes as Near-Infrared Fluorescent Molecules. *Nano Lett.* **2008**, *8*, 586–90.
- (10) Godin, A. G.; Varela, J. A.; Gao, Z.; Danné, N.; Dupuis, J. P.; Lounis, B.; Groc, L.; Cognet, L. Single-Nanotube Tracking Reveals the Nanoscale Organization of the Extracellular Space in the Live Brain. *Nat. Nanotechnol.* **2017**, *12*, 238–243.
- (11) Smith, A. M.; Mancini, M. C.; Nie, S. Bioimaging: Second Window for in Vivo Imaging. *Nat. Nanotechnol.* **2009**, *4*, 710–1.
- (12) Lim, Y. T.; Kim, S.; Nakayama, A.; Stott, N. E.; Bawendi, M. G.; Frangioni, J. V. Selection of Quantum Dot Wavelengths for Biomedical Assays and Imaging. *Mol. Imaging* **2003**, *2*, 50–64.
- (13) Welsher, K.; Liu, Z.; Sherlock, S. P.; Robinson, J. T.; Chen, Z.; Daranciang, D.; Dai, H. A Route to Brightly Fluorescent Carbon Nanotubes for Near-Infrared Imaging in Mice. *Nat. Nanotechnol.* **2009**, *4*, 773–80.
- (14) Welsher, K.; Sherlock, S. P.; Dai, H. Deep-Tissue Anatomical Imaging of Mice Using Carbon Nanotube Fluorophores in the Second Near-Infrared Window. *Proc. Natl. Acad. Sci. U. S. A.* **2011**, *108*, 8943–8948.
- (15) Ernst, F.; Heek, T.; Setaro, A.; Haag, R.; Reich, S. Energy Transfer in Nanotube-Perylene Complexes. *Adv. Funct. Mater.* **2012**, *22*, 3921–3926.
- (16) Frey, H.; Haag, R. Dendritic Polyglycerol: A New Versatile Biocompatible Material. *Rev. Mol. Biotechnol.* **2002**, *90*, 257–267.
- (17) Wyszogrodzka, M.; Haag, R. A Convergent Approach to Biocompatible Polyglycerol "Click" Dendrons for the Synthesis of Modular Core-Shell Architectures and their Transport Behavior. *Chem. - Eur. J.* **2008**, *14*, 9202–14.
- (18) Wyszogrodzka, M.; Haag, R. Study of Single Protein Adsorption onto Monoamino Oligoglycerol Derivatives: A Structure-Activity Relationship. *Langmuir* **2009**, *25*, 5703–12.
- (19) Wyszogrodzka, M.; Haag, R. Synthesis and Characterization of Glycerol Dendrons, Self-Assembled Monolayers on Gold: A Detailed Study of their Protein Resistance. *Biomacromolecules* **2009**, *10*, 1043–54.
- (20) Ernst, F.; Heek, T.; Setaro, A.; Haag, R.; Reich, S. Excitation Characteristics of Different Energy Transfer in Nanotube-Perylene Complexes. *Appl. Phys. Lett.* **2013**, *102*, 233105–9.
- (21) Ghosh, S.; Bachilo, S. M.; Simonette, R. A.; Beckingham, K. M.; Weisman, R. B. Oxygen Doping Modifies Near-Infrared Band Gaps in Fluorescent Single-Walled Carbon Nanotubes. *Science* **2010**, *330*, 1656–1660.
- (22) Ernst, F.; Heek, T.; Setaro, A.; Haag, R.; Reich, S. Functional Surfactants for Carbon Nanotubes: Effects of Design. *J. Phys. Chem. C* **2013**, *117*, 1157–1162.
- (23) Wong, C. Y.; Curutchet, C.; Tretiak, S.; Scholes, G. D. Ideal Dipole Approximation Fails to Predict Electronic Coupling and Energy Transfer Between Semiconducting Single-Wall Carbon Nanotubes. *J. Chem. Phys.* **2009**, *130*, 81104–7.
- (24) Wu, P. G.; Brand, L. Resonance Energy Transfer: Methods and Applications. *Anal. Biochem.* **1994**, *218*, 1–13.
- (25) Setaro, A.; Adeli, M.; Glaeske, M.; Przyrembel, D.; Bisswanger, T.; Gordeev, G.; Maschietto, F.; Faghani, A.; Paulus, B.; Weinelt, M.; et al. Preserving  $\pi$ -Conjugation in Covalently Functionalized Carbon Nanotubes for Optoelectronic Applications. *Nat. Commun.* **2017**, *8*, 14281–7.
- (26) Alvarez, L.; Fall, F.; Belhboub, A.; Le Parc, R.; Almadori, Y.; Arenal, R.; Aznar, R.; Dieudonné-George, P.; Hermet, P.; Rahmani, A.; et al. One-Dimensional Molecular Crystal of Phthalocyanine Confined into Single-Walled Carbon Nanotubes. *J. Phys. Chem. C* **2015**, *119*, 5203–5210.
- (27) Ayala, P.; Arenal, R.; Loiseau, A.; Rubio, A.; Pichler, T. The Physical and Chemical Properties of Heteronanotubes. *Rev. Mod. Phys.* **2010**, *82*, 1843–1885.
- (28) Arenal, R.; Blase, X.; Loiseau, A. Boron-Nitride and Boron-Carbonitride Nanotubes: Synthesis, Characterization and Theory. *Adv. Phys.* **2010**, *59*, 101–179.
- (29) Alvarez, L.; Almadori, Y.; Babaa, R.; Michel, T.; Le Parc, R.; Bantignies, J.-L.; Jusselme, B.; Palacin, S.; Hermet, P.; et al. Charge Transfer Evidence between Carbon Nanotubes and Encapsulated Conjugated Oligomers. *J. Phys. Chem. C* **2011**, *115*, 11898–11905.
- (30) Arenal, R.; De Matteis, L.; Custardoy, L.; Mayoral, A.; Tence, M.; Grazu, V.; De La Fuente, J. M.; Marquina, C.; Ibarra, M. R. Spatially-Resolved EELS Analysis of Antibody Distribution on Biofunctionalized Magnetic Nanoparticles. *ACS Nano* **2013**, *7*, 4006–13.
- (31) Wilson, A. P. Cytotoxicity and Viability. In *Animal Cell Culture: A Practical Approach*, 3rd ed.; Masters, J. R. W., Ed.; Oxford University Press: Oxford, 2000; p 190.
- (32) Jeanguillaume, C.; Colliex, C. Spectrum-Image: The Next Atep in EELS Digital Acquisition and Processing. *Ultramicroscopy* **1989**, *28*, 252–257.
- (33) Arenal, R.; de la Peña, F.; Stéphan, O.; Walls, M.; Tencé, M.; Loiseau, A.; Colliex, C. Extending the Analysis of EELS Spectrum-Imaging Data, from Elemental to Bond Mapping in Complex Nanostructures. *Ultramicroscopy* **2008**, *109*, 32–8.